**Atmospheric
Chemistry
and Physics
Discussions**

Investigating relationships between aerosol optical depth and cloud fraction using satellite, aerosol reanalysis and general circulation model data

B. S. Grandey[1,*], P. Stier[1], and T. M. Wagner[1]

[1]Atmospheric, Oceanic and Planetary Physics, Department of Physics, University of Oxford, UK
[*]now at: Singapore-MIT Alliance for Research and Technology, Singapore

Correspondence to: B. S. Grandey (benjamin@smart.mit.edu)

ACPD

12, 30805–30823, 2012

Aerosol and cloud fraction

B. S. Grandey et al.

Title Page

Abstract	Introduction
Conclusions	References
Tables	Figures

◀◀   ▶▶

◀   ▶

Back   Close

Full Screen / Esc

Printer-friendly Version

Interactive Discussion

Abstract

Strong positive relationships between cloud fraction (f_c) and aerosol optical depth (τ) have been reported. Data retrieved from the MODerate resolution Imaging Spectroradiometer (MODIS) instrument show positive f_c–τ relationships across most of the globe. However, these relationships are not necessarily due to cloud–aerosol interactions. Using state of the art Monitoring Atmospheric Composition and Climate (MACC) reanalysis-forecast τ data, which should be less affected by retrieval artifacts, it is demonstrated that a large part of the observed f_c–τ signal may be due to cloud contamination of satellite-retrieved τ. For longer MACC forecast time-steps of 24 h, which likely contain less residual cloud contamination, some negative f_c–τ relationships are found. ECHAM5-HAM general circulation model (GCM) simulations further demonstrate that positive f_c–τ relationships may arise due to covariation with relative humidity. Widespread negative simulated f_c–τ relationships in the tropics are shown to arise due to scavenging of aerosol by precipitation. Wet scavenging events are likely poorly sampled in satellite-retrieved data. Quantifying the role of wet scavenging, and assessing GCM representations of this important process, remains a challenge for future observational studies of aerosol–cloud–precipitation interactions.

1 Introduction

Microphysical and dynamical interactions between aerosols and clouds are associated with some of the largest uncertainties in projections of future climate (Lohmann and Feichter, 2005; Forster et al., 2007). One proposed aerosol effect on clouds is the cloud lifetime effect (Albrecht, 1989): increasing aerosol concentrations may decrease cloud droplet size, suppressing precipitation and enhancing the retention of liquid water by the cloud, hence increasing the lifetime of the cloud and the total cloud fractional cover. Positive relationships between satellite-retrieved cloud fraction (f_c) and aerosol optical depth (τ) have been reported and have been interpreted to indicate aerosol

cloud lifetime effects (e.g. Koren et al., 2005; Kaufman et al., 2005; Yuan et al., 2011). However, these f_c–τ relationships may not be due to aerosol effects on clouds. Many possible reasons for observed relationships between aerosol and cloud properties exist. Expanding on Quaas et al. (2010), of particular relevance to the f_c–τ relationships are the following potential mechanisms:

1. Climatological spatial gradient effects may lead to spurious f_c–τ relationships if data are analysed on large regional scales (Grandey and Stier, 2010).

2. Satellite data errors may lead to positive f_c–τ relationships. Pixels in thin and broken cloud fields, with high f_c, may be mistakenly flagged as cloud-free when they are contaminated by cloud, leading to erroneously high τ retrievals (Huang et al., 2011). Furthermore, three-dimensional scattering of light by inhomogeneous clouds may also lead to erroneously high τ retrievals (Várnai and Marshak, 2009). A possible way to avoid these problems may be to combine satellite-retrieved f_c data with simulated τ data. For example, Koren et al. (2010) combine chemical transport model τ data with MODerate resolution Imaging Spectroradiometer (MODIS) cloud data when investigating deep convective clouds over the Atlantic ocean. General circulation model (GCM) data should not suffer from this problem.

3. The simple aerosol cloud lifetime effect conceptual model would predict positive f_c–τ relationships (Albrecht, 1989), assuming τ is a suitable surrogate for cloud condensation nuclei concentration (CCN; Andreae, 2009). Many GCMs attempt to simulate this effect by coupling aerosol to the autoconversion scheme in stratiform cloud microphysics schemes, an effect that can often be switched on or off, although a large model error may exist.

4. Relative humidity may drive positive f_c–τ relationships (Quaas et al., 2010; Chand et al., 2012). Cloud fraction generally increases with relative humidity. Aerosols swell hygroscopically in high relative humidity conditions, increasing τ. GCMs

should be able to reproduce this effect, particularly as cloud cover parameterizations are generally heavily dependent on relative humidity (e.g. Sundqvist et al., 1989), although there may be significant model errors. GCM-modelled dry τ, which assumes no hygroscopic aerosol growth and may therefore be a better surrogate for the CCN which would be activated at a given supersaturation, allows for this relative humidity effect to be accounted for, as demonstrated by Quaas et al. (2010). Chand et al. (2012) have recently used a Gaussian probability density function model to show that observed f_c–τ relationships are consistent with hygroscopic growth of aerosol.

5. Other meteorological factors may lead to spurious f_c–τ relationships. For example, 10-m wind speed is capable of explaining a significant part of observed f_c–τ relationships over ocean (Engström and Ekman, 2010). This is because τ increases with 10-m wind speed over ocean likely due to both sea-surface brightness contamination of the τ retrieval and genuine wind speed dependent emission of seasalt (Grandey et al., 2011), and higher f_c values are likely found for meteorological conditions associated with higher wind speeds. GCMs should be capable of reproducing meteorological effects.

6. Wet scavenging of aerosols by precipitation might lead to negative f_c–τ relationships, assuming a positive correlation between f_c and precipitation. GCM aerosol modules simulate wet scavenging as the major removal mechanism for atmospheric aerosol.

7. Cloud processing of aerosols may alter the optical properties of aerosols. Far away from sources, aerosol particles may have been cycled through clouds approximately three times (Pruppacher and Jaenicke, 1995).

In order to investigate some of these possible mechanisms, two additional tools are used in this paper alongside Aqua-MODIS data. Firstly, Monitoring Atmospheric Composition and Climate (MACC) project reanalysis-forecast τ data are used in an attempt

Title Page

Abstract | Introduction

Conclusions | References

Tables | Figures

◄ | ►►

◄ | ►

Back | Close

Full Screen / Esc

Printer-friendly Version

Interactive Discussion

to investigate cloud contamination errors in the MODIS τ data (second point above). Secondly, the ECHAM5-HAM GCM is used to investigate the cloud lifetime effect, relative humidity and wet scavenging contributions (third, fourth and sixth points above).

The following questions are asked in this paper: to what extent may cloud contamination errors be responsible for the observed f_c–τ relationships? What are the dominant physical processes leading to genuine f_c–τ relationships?

2 Method

The satellite data used in this paper are from the official Aqua-MODIS science team Collection 5 level 3 daily 1° × 1° cloud and aerosol dataset (MYD08_D3) (Platnick et al., 2003; Remer et al., 2005). Total cloud fraction (f_c) and aerosol optical depth at 550 nm (τ) are of interest here.

As mentioned above, cloud contamination of τ retrievals may cause spurious f_c–τ relationships, something that may be avoidable by pairing satellite-derived f_c with τ from a state of the art reanalysis-forecast aerosol dataset. However, residual cloud contamination may remain and model errors may be introduced. The reanalysis-forecast τ data used in this paper are from the MACC project (Morcrette et al., 2011). The model uses a mixed bulk and bin aerosol scheme (Morcrette et al., 2009). MODIS Collection 5 τ data are assimilated using a 4D-Var scheme with a 12 h assimilation window (Benedetti et al., 2009). Further discussion of the MACC data, including comparisons with satellite-retrieved and AErosol RObotic NETwork (AERONET) aerosol data, is provided in Morcrette et al. (2011). MACC data from two different forecast time-steps, relative to the most recent assimilation time of 00:00 UTC, are used: $t + 3$ h; $t + 24$ h from assimilation the previous day. The $t + 24$ h τ is likely to have less residual cloud contamination but more model bias than the $t + 3$ h τ. Since the MACC τ data approximately correspond to the start of each day, they are temporally interpolated equally between each pair of days, corresponding to interpolation times of 15 UTC for $t + 3$ h and 12:00 UTC for $t + 24$ h. It is assumed that the interpolated τ is representative of

the τ at the Aqua daytime equatorial overpass time of 13:30 LT. The MACC data are spatially interpolated from 1.125° × 1.125° to 1° × 1° in order to match the MODIS data. The MODIS and MACC data used in this paper cover 2003–2007.

Data from the ECHAM5 GCM with the HAM aerosol model are also used (Stier et al., 2005; Zhang et al., 2012). The HAM aerosol model has been coupled to the two-moment cloud microphysics via activation of cloud droplets, droplet number dependent autoconversion and the impact of the effective radius on the cloud radiative properties, allowing the cloud albedo and cloud lifetime aerosol effects to be represented (Lohmann et al., 2007; Stier et al., 2012). Of particular interest here is the cloud lifetime effect on f_c. Six simulations are performed. Three of these use the Sundqvist cloud cover scheme, which parameterizes f_c using relative humidity as the only input (Sundqvist et al., 1989); three use the statistical Tompkins cloud cover scheme, which uses a prognostic probability density function of water vapour, considering processes such as convection, turbulence and microphysics (Tompkins, 2002). For each cloud cover scheme, three simulations are conducted: a Control run, with aerosol indirect effects represented; a NoAIE run, with no aerosol indirect effects (fixed cloud droplet number concentration); and a NoConvScav run, with aerosol indirect effects represented but with no convective wet scavenging of aerosols. Only the results for the Sundqvist simulations are presented in this main body of this paper. The results for the Tompkins simulations, which are very similar to those for the Sundqvist simulations, can be viewed in the Supplement. As in Zhang et al. (2012), all simulations use year 2000 present-day aerosol and precursor emissions, are nudged to year 2000 meteorology using European centre for medium range weather forecasts reanalysis (ERA-40) data, and are preceded by a three month spin-up period from October 1999. All simulations are run at T63 horizontal resolution, corresponding to 1.875° × 1.875°, and L31 vertical resolution. Aerosol and cloud data are output at six hour resolution. The f_c data are calculated assuming maximum-random overlap of cloud layers, using an updated version of the satellite simulator module used in Quaas et al. (2009) (Stier et al., 2012). In addition to τ from all simulations, dry τ output from the Control simulations is also used.

Title Page

Abstract | Introduction

Conclusions | References

Tables | Figures

⏮ | ⏭

◀ | ▶

Back | Close

Full Screen / Esc

Printer-friendly Version

Interactive Discussion

Following Quaas et al. (2010), dry τ is diagnosed by reducing the extinction coefficient of each aerosol mode by the volume fraction of water for that mode, approximating the τ that would be calculated if there was no hygroscopic swelling of the aerosols.

The f_c data are categorized into two cases: low τ conditions, where τ is less than the median for that grid-box, season and dataset; high τ conditions, where τ is greater than the median. The mean f_c for each grid-box, season and dataset is then calculated for low τ and high τ conditions, before averaging across all four seasons to produce annual mean fields. The difference in f_c between low and high conditions is then calculated. The analysis is limited to 60° S–60° N.

3   Results and discussion

Figure 1 shows the difference in f_c between low and high τ conditions. Positive f_c–τ relationships, shown in red, are found globally. Positive f_c–τ relationships have been observed in other studies, such as those by Koren et al. (2005) and Kaufman et al. (2005) who investigated clouds over the North Atlantic ocean using earlier MODIS data. Particularly strong relationships, shown in darker shades of red, are found over the subtropical oceans, Southern South America and Eastern North America. The relationship over the extratropical southern oceans is weaker. Over ocean, there is a mean increase in f_c of 0.20 from 0.51 to 0.71; over land, there is also a mean increase of 0.20 from 0.30 to 0.50.

An increase of 0.2 in f_c is relatively large. For example, assuming an idealised ocean albedo of 0.0 and a cloud albedo of 0.5, a 0.2 increase in f_c may lead to an albedo increase of order 0.1 over ocean. Given a solar constant of $1370\,\mathrm{W\,m^{-2}}$, averaged to $340\,\mathrm{W\,m^{-2}}$ across the surface of the earth, an albedo increase of 0.1 would correspond to a shortwave radiation decrease of order $30\,\mathrm{W\,m^{-2}}$ at the top of the atmosphere. Of course, this shortwave decrease might be offset be a sizeable longwave increase, particularly if the cover of high clouds increases.

Full Screen / Esc

Printer-friendly Version

Interactive Discussion

In Chapter 3 of Grandey (2011), two other satellite datasets (Clouds and Earth's Radiant Energy System Single Scanner Footprint; and Advanced-Along Track Scanning Radiometer GlobAEROSOL τ data with Oxford-RAL Retrieval of Aerosol and Clouds f_c data) were also investigated. It was shown that positive f_c–τ relationships also exist for these datasets, although the relationships are not as strong as in the Aqua-MODIS Collection 5 data.

As previously stated, the positive f_c–τ relationships are not necessarily due to aerosol indirect effects on cloud. Cloud contamination of aerosol retrievals provides one potential explanation. In an attempt to investigate this error, the MODIS f_c data are paired with MACC reanalysis-forecast τ data, a combination henceforth referred to as MODIS–MACC. The results of categorising according to low and high MACC $t + 3\,\text{h}$ τ conditions are shown in Fig. 2a. Globally positive f_c–τ relationships are again evident, although they are generally weaker than cases when MODIS τ is used. For a few small regions, notably part of the extratropical South Atlantic ocean, weak negative f_c–τ relationships are observed, indicated by pale blue. Over ocean, the global mean increase is now 0.13; over land, the increase is 0.15.

Residual cloud contamination may remain in the MACC τ data due to the assimilation of satellite-retrieved τ. This contamination should decrease for longer forecast times from assimilation, although model bias will increase as the forecast length increases. The MODIS–MACC f_c–τ relationships for a longer MACC forecast of $t + 24\,\text{h}$ are shown in Fig. 2b. The relationships are generally weaker than for $t + 3\,\text{h}$, although the spatial patterns are similar. Negative f_c–τ relationships are more evident in the tropics for the $t + 24\,\text{h}$ τ data. Over ocean, the global mean increase is 0.09; over land, the increase is 0.12. Assuming that the MACC $t + 24\,\text{h}$ τ data do not contain model bias or residual cloud contamination, this suggests that cloud contamination may account for approximately one half of the observed global increase in f_c over ocean. However, it is difficult to disentangle the contributions from residual cloud contamination and introduced model bias.

It is worth noting that MODIS τ retrievals do not exist for completely cloudy grid boxes, whereas MACC τ data exist everywhere. Sampling differences such as these may be important (Sayer et al., 2010). When MACC $t + 24$ h τ data are sampled according to Aqua-MODIS τ availability, fewer grid-boxes show negative relationships. However, sampling choice does not have a large impact globally (Fig. S1a, b of the Supplement).

Results for the ECHAM5-HAM Sundqvist Control simulation are shown in Fig. 2c. The spatial distribution of positive and negative relationships is remarkably similar between the Sundqvist Control and the MODIS–MACC $t + 24$ h results. The strong positive f_c–τ relationships observed over the subtropical oceans, Southern South America, North America, Asia and Australia are of similar size to those for the MODIS–MACC combinations. Further agreement is found in the extratropical ocean, where the relationships are weaker, with some weak negative relationships in the extratropical southern oceans. As observed in the MODIS–MACC $t+24$ h data, negative f_c–τ relationships are found over parts of the tropics, particularly South-East Asia, although these negative relationships are much stronger in the Sundqvist Control data. These negative relationships, which occur primarily over the tropical ocean, greatly reduce the global mean increase in f_c to 0.03 over ocean. Over land, the global mean increase is 0.11, comparable to the MODIS–MACC $t + 24$ h results.

Seven possible mechanisms for f_c–τ relationships were suggested at the beginning of this paper. The first of these, namely spatial gradient effects, has been avoided by conducting the analysis on small regions of $1° \times 1°$ or $1.875° \times 1.875°$. The second of these, namely cloud contamination of τ, is difficult to remove from the satellite data, although an attempt has been made to investigate this error by using MACC τ. Cloud contamination does not impact the ECHAM5-HAM model results. Four possible mechanisms remain for explaining the ECHAM5-HAM Sundqvist Control results. Two of these would predict positive f_c–τ relationships: the aerosol cloud lifetime effect and hygroscopic growth of aerosol in high relativity humidity conditions. One would predict negative f_c–τ relationships: wet scavenging of aerosol by precipitation. The contributions

of these three effects to the ECHAM5-HAM Sundqvist Control results are now investigated. The two remaining possible mechanisms, whereby spurious f_c–τ relationships are caused by other meteorological factors or cloud processing of aerosols, are not tested here.

First, the contribution of the cloud lifetime effect is investigated. The Control simulation contains a representation of the cloud albedo and cloud lifetime effects, assuming the cloud lifetime effect can be represented through a modulation of autoconversion only. These aerosol indirect effects are not included in the NoAIE simulation. The difference in f_c between low and high τ conditions for the NoAIE simulation is shown in Fig. 2d. A slight weakening of positive f_c–τ relationships occurs over many subtropical ocean areas, and the differences in the Southern Indian Ocean become more negative. However, a slight strengthening of positive f_c–τ relationships occurs over land for the NoAIE run, opposite from what would be expected from the conceptual cloud lifetime effect. These results suggest that the model simulated indirect effects are not the primary mechanism responsible for the positive f_c–τ relationships observed in the Control simulation. This is consistent with the findings of Lohmann et al. (2006) and Quaas et al. (2010).

Second, the contribution of relative humidity is investigated. In order to do this, dry τ from the Control simulation is used instead of total τ. Dry τ provides a surrogate for the CCN which would be activated at a given supersaturation but which is independent of relative humidity. Because τ is heavily dependent on aerosol size, dry τ is generally much lower than τ (Fig. S2a, b). The f_c difference between low and high dry τ conditions in the Control run are shown in Fig. 2e. It can be clearly seen that using dry τ removes the majority of the positive f_c–τ relationships over ocean. Many land areas retain positive f_c–dry τ relationships. However, these positive relationships are significantly weakened compared to when total τ is used. A global mean negative f_c–dry τ relationship is found over both ocean and land. These results demonstrate that relative humidity is the primary driver for the positive f_c–τ relationships, in agreement with Quaas et al. (2010) and Chand et al. (2012).

Third, the contribution of wet scavenging is investigated. The negative f_c–τ relationships in the Control run are generally found in the tropics, where convective precipitation dominates, constituting 95 % of the 20° S–20° N precipitation in the Control simulation. It is these negative relationships which are of interest here, so wet scavenging by convective precipitation is switched off for the NoConvScav simulation, although the convective precipitation itself remains. Scavenging by stratiform cloud precipitation remains. Wet scavenging is the major removal mechanism for aerosol in ECHAM5-HAM. As a result, τ is generally much higher in the the NoConvScav simulation compared to the Control simulation, particularly in the tropics (Fig. S2c). The lifetime of aerosols in ECHAM5-HAM is typically less than a week when scavenging is turned on (Stier et al., 2005). Switching off convective scavenging increases τ by a factor of approximately three, suggesting a lifetime of less than three weeks for the NoConvScav simulation. Therefore the three month spin-up should allow these concentrations to reach an equilibrium by the start of the year 2000 analysis period. Figure 2f shows the results for the NoConvScav simulation. Most of the negative f_c–τ relationships found in the tropics of the Control simulation are removed, becoming positive in the NoConvScav simulation. This demonstrates that wet scavenging by convective precipitation is the primary reason for the strong negative f_c–τ relationships found in the tropics of the Control simulation. Interestingly, the f_c–τ relationships become more negative for many extratropical ocean areas in the NoConvScav simulation compared to the Control simulation. This may be because wet scavenging by stratiform cloud precipitation may become a more significant aerosol removal mechanism in the NoConvScav run, leading to more negative relationships in regions where stratiform precipitation dominates.

Since τ cannot be retrieved in cloudy conditions, passive satellite radiometers such as MODIS may have poor sampling of negative f_c–τ relationships arising due to scavenging. This may partly explain the absence of negative relationships in the Aqua-MODIS data, and also the reduction in the number of grid-boxes with negative relationships when sampling is applied to the MODIS–MACC $t + 24$ h data. Although some negative relationships are observed for MODIS–MACC $t + 24$ h, the MODIS–MACC

Aerosol and cloud fraction

B. S. Grandey et al.

Full Screen / Esc

Printer-friendly Version

Interactive Discussion

combination may underestimate the negative relationships due to differences between modelled precipitation and real precipitation for a given location and day.

The results for simulations where the Tompkins stratiform cloud cover scheme is used are similar to those for the Sundqvist results described above (Fig. S1c–f in the Supplement). The results for two alternative methods of quantifying the f_c–τ relationships, namely $\frac{\mathrm{d}f_c}{\mathrm{d}\ln\tau}$ gradients and correlations, are shown in Figs. S3 and S4 in the Supplement. Similar conclusions can be reached using these figures, showing that the findings presented in this study appear to be insensitive to different methods of quantifying the f_c–τ relationships.

4   Conclusions

Strong positive relationships between retrieved f_c and τ are observed in Aqua-MODIS satellite data. A global mean f_c increase of 0.20 between low and high conditions is found for both ocean and land.

Categorising the Aqua-MODIS f_c data according to MACC reanalysis-forecast $t + 3\,\mathrm{h}$ τ data results in a general weakening of the observed positive f_c–τ relationships. The positive relationships are weakened further for a longer MACC forecast period of $t + 24\,\mathrm{h}$. This provides some evidence to suggest that part of the positive f_c–τ relationships observed in the MODIS data may be due to retrieval errors, although the weakening of the relationships may also be due to MACC model errors. Positive f_c–τ relationships are still observed to dominate globally for the MODIS–MACC combinations, particularly in the subtropics. However, negative relationships emerge over parts of the tropics and extratropical southern oceans in the $t + 24\,\mathrm{h}$ data.

The results of ECHAM5-HAM Control simulations generally agree well with the MODIS–MACC results in the subtropics and extratropics. In agreement with the MODIS–MACC $t + 24\,\mathrm{h}$ results, negative f_c–τ relationships are found in parts of the tropics. However, these negative relationships are found to be much stronger in the ECHAM5-HAM Control simulations. NoAIE simulations, in which simulated aerosol

indirect effects have been switched off, demonstrate that the cloud lifetime effect is not the primary contributor to positive f_c–τ relationships in ECHAM5-HAM. Rather, the positive relationships are primarily due to hygroscopic swelling of aerosols in high relative humidity conditions, demonstrated by using dry τ instead of total τ. NoConvScav simulations, in which convective wet scavenging has been switched off, demonstrate that the negative f_c–τ relationships in the tropics are primarily due to wet scavenging by convective precipitation. These results demonstrate the important contribution of wet scavenging to aerosol–cloud interactions.

Wet scavenging events are likely poorly sampled in retrieved satellite data, due to the absence of τ retrievals in cloudy conditions. This may partly explain why negative relationships are not observed in the Aqua-MODIS data. Similarly, this may also explain an absence of negative relationships between retrieved rain rate and τ (Koren et al., 2012). Quantifying the role of wet scavenging, and assessing GCM representations of this process, remains a challenge for future observational studies of aerosol–cloud–precipitation interactions.

It would be beneficial if the findings presented here were to be further analysed in future studies using different tools and methodologies. In particular, analysing f_c–τ relationships for different cloud regimes may provide further insight. Such a regime-based approach has already been applied to the investigation of relationships between τ and cloud droplet number concentration (Gryspeerdt and Stier, 2012). Large-scale synoptic conditions, so as those associated with extratropical cyclones, can also be considered (Grandey et al., 2012). It would also be beneficial to identify the reasons for f_c–τ relationships in other global model datasets. The GCM results can be supplemented by cloud-resolving models, which are more accurate tools for the investigation of cloud-scale processes for specific regimes and geographical regions.

Supplementary material related to this article is available online at: http://www.atmos-chem-phys-discuss.net/12/30805/2012/ acpd-12-30805-2012-supplement.pdf.

Title Page

Abstract | Introduction

Conclusions | References

Tables | Figures

◄ | ►

◄ | ►

Back | Close

Full Screen / Esc

Printer-friendly Version

Interactive Discussion

References

Albrecht, B. A.: Aerosols, cloud microphysics, and fractional cloudiness, Science, 245, 1227–1230, 1989. 30806, 30807

Andreae, M. O.: Correlation between cloud condensation nuclei concentration and aerosol optical thickness in remote and polluted regions, Atmos. Chem. Phys., 9, 543–556, doi:10.5194/acp-9-543-2009, 2009. 30807

Benedetti, A., Morcrette, J.-J., Boucher, O., Dethof, A., Engelen, R. J., Fisher, M., Flentje, H., Huneeus, N., Jones, L., Kaiser, J. W., Kinne, S., Mangold, A., Razinger, M., Simmons, A. J., and Suttie, M.: Aerosol analysis and forecast in the European Centre for Medium-Range Weather Forecasts Integrated Forecast System: 2. Data assimilation, J. Geophys. Res., 114, D13205, doi:10.1029/2008JD011115, 2009. 30809

Chand, D., Wood, R., Ghan, S. J., Wang, M., Ovchinnikov, M., Rasch, J. P., Miller, S., Schichtel, B., and Moore, T., Aerosol optical depth increase in partly cloudy conditions, J. Geophys. Res., 117, D17207, doi:10.1029/2012JD017894, 2012. 30807, 30808, 30814

Engström, A. and Ekman, A. M. L.: Impact of meteorological factors on the correlation between aerosol optical depth and cloud fraction, Geophys. Res. Lett., 37, L18814, doi:10.1029/2010GL044361, 2010. 30808

Forster, P., Ramaswamy, V., Artaxo, P., Berntsen, T., Betts, R., Fahey, W. D., Haywood, J., Lean, J., Lowe, D. C., Myhre, G., Nganga, J., Prinn, R., Raga, G., Schultz, M., and Van Dorland, R.: Changes in atmospheric constituents and in radiative forcing, in: Climate Change 2007: The Physical Science Basis, Contribution of Working Group 1 to the Fourth

Assessment Report of the Intergovernmental Panel on Climate Change, Cambridge University Press, 2007. 30806

Grandey, B. S.: Investigating aerosol–cloud interactions, PhD thesis, University of Oxford, UK, available at: http://ora.ox.ac.uk/objects/uuid:8b48c02b-3d43-4b04-ae55-d9885960103d, 2011. 30812

Grandey, B. S. and Stier, P.: A critical look at spatial scale choices in satellite-based aerosol indirect effect studies, Atmos. Chem. Phys., 10, 11459–11470, doi:10.5194/acp-10-11459-2010, 2010. 30807

Grandey, B. S., Stier, P., Wagner, T. M., Grainger, R. G., and Hodges, K. I.: The effect of extra-tropical cyclones on satellite-retrieved aerosol properties over ocean, Geophys. Res. Lett., 38, L13805, doi:10.1029/2011GL047703, 2011. 30808

Grandey, B. S., Stier, P., Grainger, R. G., and Wagner, T. M.: The contribution of extratropical cyclones to observed cloud–aerosol relationships, in preparation, 2012. 30817

Gryspeerdt, E. and Stier, P.: Regime-based analysis of aerosol–cloud interactions, Geophys. Res. Lett., 39, L21802, doi:10.1029/2012GL053221, 2012. 30817

Huang, J., Hsu, N. C., Tsay, S.-C., Jeong, M.-J., Holben, B. N., Berkoff, T. A., and Welton, E. J.: Susceptibility of aerosol optical thickness retrievals to thin cirrus contamination during the BASE-ASIA campaign, J. Geophys. Res., 116, D08214, doi:10.1029/2010JD014910, 2011. 30807

Kaufman, Y. J., Koren, I., Remer, L. A., Rosenfeld, D., and Rudich, Y.: The effect of smoke, dust, and pollution aerosol on shallow cloud development over the Atlantic Ocean, P. Natl. Acad. Sci. USA, 102, 11207–11212, doi:10.1073/pnas.0505191102, 2005. 30807, 30811

Koren, I., Kaufman, Y. J., Rosenfeld, D., Remer, L. A., and Rudich, Y.: Aerosol invigoration and restructuring of the Atlantic convective clouds, Geophys. Res. Lett., 32, L14828, doi:10.1029/2005GL023187, 2005. 30807, 30811

Koren, I., Feingold, G., and Remer, L. A.: The invigoration of deep convective clouds over the Atlantic: aerosol effect, meteorology or retrieval artifact?, Atmos. Chem. Phys., 10, 8855–8872, doi:10.5194/acp-10-8855-2010, 2010. 30807

Koren, I., Altaratz, O., Remer, L. A., Feingold, G., Martins, J. V., and Heiblum, R. H.: Aerosol-induced intensification of rain from the tropics to the mid-latitudes, Nat. Geosci., 5, 118–122, doi:10.1038/NGEO1364, 2012. 30817

Lohmann, U. and Feichter, J.: Global indirect aerosol effects: a review, Atmos. Chem. Phys., 5, 715–737, doi:10.5194/acp-5-715-2005, 2005. 30806

Title Page

Abstract | Introduction

Conclusions | References

Tables | Figures

◀◀ | ▶▶

◀ | ▶

Back | Close

Full Screen / Esc

Printer-friendly Version

Interactive Discussion

Lohmann, U., Koren, I., and Kaufman, Y. J.: Disentangling the role of microphysical and dynamical effects in determining cloud properties over the Atlantic, Geophys. Res. Lett., 33, L09802, doi:10.1029/2005GL024625, 2006. 30814

5 Lohmann, U., Stier, P., Hoose, C., Ferrachat, S., Kloster, S., Roeckner, E., and Zhang, J.: Cloud microphysics and aerosol indirect effects in the global climate model ECHAM5-HAM, Atmos. Chem. Phys., 7, 3425–3446, doi:10.5194/acp-7-3425-2007, 2007. 30810

Morcrette, J.-J., Boucher, O., Jones, L., Salmond, D., Bechtold, P., Beljaars, A., Benedetti, A., Bonet, A., Kaiser, J. W., Razinger, M., Schulz, M., Serrar, S., Simmons, A. J., Sofiev, M.,

10 Suttie, M., Tompkins, A. M., and Untch, A.: Aerosol analysis and forecast in the European centre for medium-range weather forecasts integrated forecast system: forward modeling, J. Geophys. Res., 114, D06206, doi:10.1029/2008JD011235, 2009. 30809

Morcrette, J.-J., Benedetti, A., Jones, L., Kaiser, J. W., Razinger, M., and Suttie, M.: Prognostic aerosols in the ECMWF IFS: MACC vs. GEMS aerosols, ECMWF Tech. Memo. 659, avail-

15 able at: http://www.ecmwf.int/publications/library/ecpublications/%5Fpdf/tm/601-700/tm659. pdf, last access: 2012-11-28, 'European Centre for Medium-Range Weather Forecasts, Reading, UK, 32 pp., 2011. 30809

Platnick, S., King, M. D., Ackerman, S. A., Menzel, W. P., Baum, B. A., Riedi, J. C., and Frey, R. A.: The MODIS cloud products: algorithms and examples from Terra, IEEET. Geosci.

20 Remote, 41, 459–473, doi:10.1109/TGRS.2002.808301, 2003. 30809

Pruppacher, H. R. and Jaenicke, R.: The processing of water vapor and aerosols by atmospheric clouds, a global estimate, Atmos. Res., 38, 283–295, 1995. 30808

Quaas, J., Ming, Y., Menon, S., Takemura, T., Wang, M., Penner, J. E., Gettelman, A., Lohmann, U., Bellouin, N., Boucher, O., Sayer, A. M., Thomas, G. E., McComiskey, A., Fein-

25 gold, G., Hoose, C., Kristjánsson, J. E., Liu, X., Balkanski, Y., Donner, L. J., Ginoux, P. A., Stier, P., Grandey, B., Feichter, J., Sednev, I., Bauer, S. E., Koch, D., Grainger, R. G., Kirkevåg, A., Iversen, T., Seland, Ø., Easter, R., Ghan, S. J., Rasch, P. J., Morrison, H., Lamarque, J.-F., Iacono, M. J., Kinne, S., and Schulz, M.: Aerosol indirect effects – general circulation model intercomparison and evaluation with satellite data, Atmos. Chem. Phys., 9,

30 8697–8717, doi:10.5194/acp-9-8697-2009, 2009. 30810

Quaas, J., Stevens, B., Stier, P., and Lohmann, U.: Interpreting the cloud cover – aerosol optical depth relationship found in satellite data using a general circulation model, Atmos. Chem. Phys., 10, 6129–6135, doi:10.5194/acp-10-6129-2010, 2010. 30807, 30808, 30811, 30814
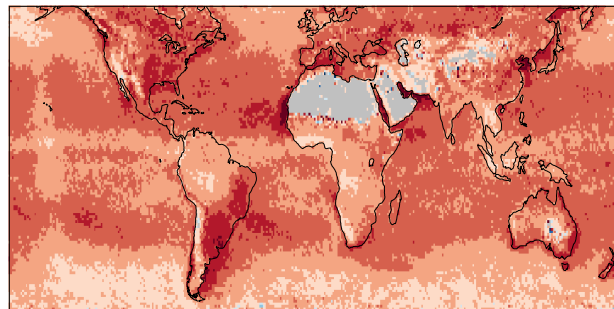
Remer, L. A., Kaufman, Y. J., Tanré, D., Mattoo, S., Chu, D. A., Martins, J. V., Li, R.-R., Ichoku, C., Levy, R. C., Kleidman, R. G., Eck, T. F., Vermote, E., and Holben, B. N.: The MODIS aerosol algorithm, products, and validation, J. Atmos. Sci., 62, 947–973, doi:10.1175/JAS3385.1, 2005. 30809

Sayer, A. M., Thomas, G. E., Palmer, P. I., and Grainger, R. G.: Some implications of sampling choices on comparisons between satellite and model aerosol optical depth fields, Atmos. Chem. Phys., 10, 10705–10716, doi:10.5194/acp-10-10705-2010, 2010. 30813

Stier, P., Feichter, J., Kinne, S., Kloster, S., Vignati, E., Wilson, J., Ganzeveld, L., Tegen, I., Werner, M., Balkanski, Y., Schulz, M., Boucher, O., Minikin, A., and Petzold, A.: The aerosol-climate model ECHAM5-HAM, Atmos. Chem. Phys., 5, 1125–1156, doi:10.5194/acp-5-1125-2005, 2005. 30810, 30815

Stier, P., Grandey, B. S., West, R., Lohmann, U., Quaas, J., and Seinfeld, J.: Observational constraints on mechanistic aerosol–cloud coupling in the microphysical aerosol-climate Model ECHAM-HAM, Atmos. Chem. Phys. Discuss., in preparation, 2012. 30810

Sundqvist, H., Berge, E., and Kristjánsson, J. E.: Condensation and cloud parameterization studies with a mesoscale numerical weather prediction model, Mon. Weather Rev., 117, 1641–1657, doi:10.1175/1520-0493(1989)117<1641:CACPSW>2.0.CO;2, 1989. 30808, 30810

Tompkins, A. M.: A prognostic parameterization for the subgrid-scale variability of water vapor and clouds in large-scale models and its use to diagnose cloud cover, J. Atmos. Sci., 59, 1917–1942, doi:10.1175/1520-0469(2002)059<1917:APPFTS>2.0.CO;2, 2002. 30810

Várnai, T. and Marshak, A.: MODIS observations of enhanced clear sky reflectance near clouds, Geophys. Res. Lett., 36, L06807, doi:10.1029/2008GL037089, 2009. 30807

Yuan, T., Remer, L. A., and Yu, H.: Microphysical, macrophysical and radiative signatures of volcanic aerosols in trade wind cumulus observed by the A-Train, Atmos. Chem. Phys., 11, 7119–7132, doi:10.5194/acp-11-7119-2011, 2011. 30807

Zhang, K., O'Donnell, D., Kazil, J., Stier, P., Kinne, S., Lohmann, U., Ferrachat, S., Croft, B., Quaas, J., Wan, H., Rast, S., and Feichter, J.: The global aerosol-climate model ECHAM-HAM, version 2: sensitivity to improvements in process representations, Atmos. Chem. Phys., 12, 8911–8949, doi:10.5194/acp-12-8911-2012, 2012. 30810
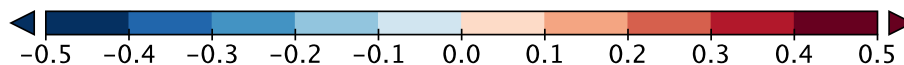
(a) Aqua-MODIS Coll. 5

Fig. 1. Annual (all seasons) mean difference (high – low) in Aqua-MODIS Collection 5 cloud fraction (f_c) between low Aqua-MODIS aerosol optical depth ($\tau <$ seasonal grid box median) conditions and high τ ($\tau >$ seasonal grid box median) conditions. Grey represents missing data.

(a) MODIS–MACC t + 3 hour   (b) MODIS–MACC t + 24 hour   (c) Sundqvist Control

(d) Sundqvist NoAIE   (e) Sundqvist Control Dry   (f) Sundqvist NoConvScav

−0.5   −0.4   −0.3   −0.2   −0.1   0.0   0.1   0.2   0.3   0.4   0.5
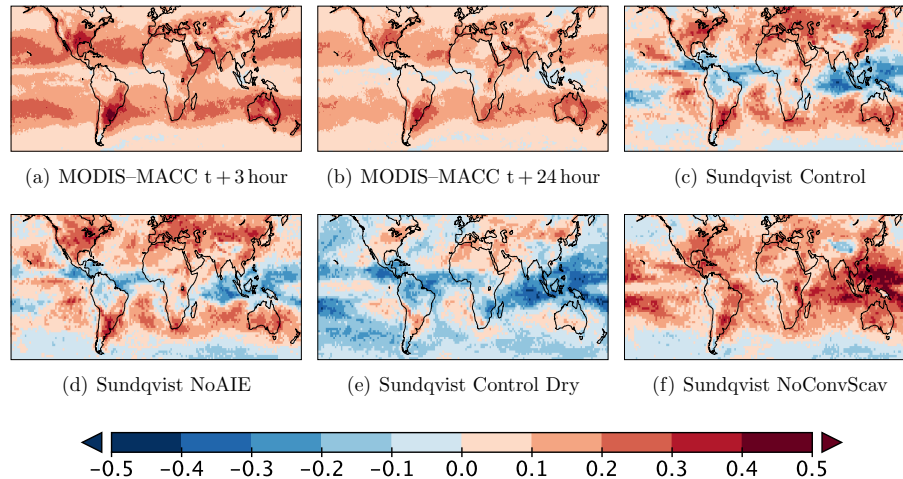
Fig. 2. Same as Fig. 1, but for **(a)** Aqua-MODIS f_c with MACC $t + 3$ τ, **(b)** Aqua-MODIS f_c with MACC $t + 24$ τ, **(c)** ECHAM5-HAM Sundqvist Control simulation f_c with τ, **(d)** Sundqvist NoAIE f_c with τ, **(e)** Sundqvist Control f_c with dry τ and **(f)** Sundqvist NoConvScav f_c with τ. Corresponding results for sampled MODIS–MACC and the ECHAM5-HAM Tompkins simulations are shown in Fig. S1 of the Supplement.